Highly efficient 3D tracking and visualization of loopless active MRI devices using slice-direction-dephased, undersampled projection imaging

A. K. George[1], J. A. Derbyshire[1], M. S. Hansen[1], C. E. Saikus[1], O. Kocaturk[1], R. J. Lederman[1], and A. Z. Faranesh[1]
[1]National Institutes of Health, Bethesda, Maryland, United States

Introduction: In MR-guided interventions accurate knowledge of the location of an interventional device (such as a catheter or guidewire) is crucial to the success of the procedure and the safety of the patient. A multi-slice, real-time MRI visualization system [1] is used in combination with *active* MR devices (devices that contain their own MR coil whose signal can be collected separately from the other coils in the scanner) to visualize the device in relation to surrounding tissue. Figure 1 shows the image of a two-channel loopless-coil active device image color-blended with the gray-scale tissue image. The advantage of a loopless-coil [2] design over looped coils [3] is that (a) it allows for improved visualization because the signal appears along an extended length of the device as opposed to along discrete points along it and (b) the coil can be used in narrower and more flexible devices. As long as the device lies within the slice it is well visualized but a common problem is that the device, while being maneuvered inside the patient, moves outside the currently imaged slice and is no longer visible to the operator.

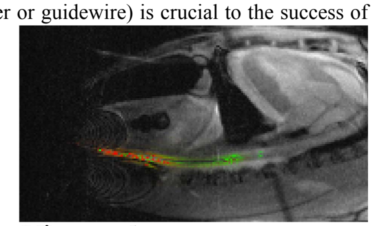
Figure 1

In this paper we present a method to efficiently track the 3D curve of a moving loopless-coil device. The goal is to do so by collecting a small amount of tracking data in between collecting data to reconstruct the slices in the multi-slice display. This 3D curve can be used to reposition the imaged slice to contain the device or be displayed in a multi-slice 3D rendering [1].

Methods to track the 3D coordinates of a looped coil [3] from a small number (~3) of 3D k-space lines do not work for a loopless-coil as they have spatially-extensive signals (i.e. curve-like as opposed to dot-like). George et al [4] demonstrated how the 3D curve of the loopless device can be reconstructed from three perpendicular MR projections (~600 ms of data) and the imaged slice can be automatically repositioned to contain the device. Their method is unsuitable for continuous tracking because of its prohibitively large data requirements. Schirra et al [5], using compressed sensing to exploit the sparsity of projection images of active device, greatly reduced the data requirements and recommend using three projections and 15 k-space lines per projection (for a total of 45 k-space lines per instance). George et al [6] presented a method that uses two projections, and a data gathering scheme which adapts the orientation and undersampling rate of those projections, and report a data requirement of 44 k-space lines per time instance.

The method we present in this abstract improves on [6] by incorporating two crucial innovations: (a) slice-direction dephasing and (b) in-plane rotation of the projection images. We present experimental results in which we are able to track the 3D curve of the device with as few as 14 total k-space lines per time-instance in the best case, 47 total k-space lines in the worst case and a median of 20 total k-space lines. In addition to the reduced data requirements over all previously presented methods, the advantage of our method over [5] is that it is computationally cheap and therefore can be implemented in real-time.

Methods: As in [6], our method adapts the orientation and undersampling-rate of the two projection images based on the knowledge of the curve of the device at the previous tracking instance. It adapts the orientation of the projections by fitting a plane to the curve of the device (computed at the previous tracking instance) and choosing the two projections to be rotated by +67 º and -67 º with respect to that plane. This choice of rotation angle provides a compromise between a projection image that is likely to have an occluded view of the device (if a 90 º rotation angle were used) and a projection image with a large field-of-view (if a 0º rotation angle were used). The projections are formed from highly undersampled Cartesian data and therefore exhibits periodic image copies along the phase-encoding direction as shown in Figure 2. The method to find the new curve succeeds as long as the image copies do not overlap with each other. The undersampling factor is chosen to be the highest possible that allows for no overlap of image-copies, while allowing for some motion of the device from the previous tracking instance to this one. The current curve of the device is estimated by adjusting the previous curve of the device to match the closest copy in the two projection images.

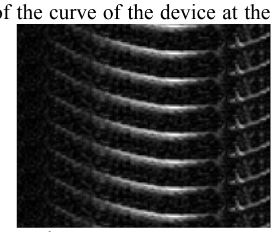
Figure 2

Figure 3 demonstrates the use of slice-direction dephasing [7,3] to improve the projection image of a loopless active device. As shown in Figure 3(a) a projection image of an active device, without dephasing, can have a bright signal far away from the curve of the device and thereby introduce errors into the curve-finding method. Figure 3(b) shows the projection image *with* slice-direction dephasing. Notice that the bright pixels of the image strictly correspond to the curve of the device. As explained in [3], the problem in Figure 3(a) is that spins that are far away from the device coherently add along the projection direction, despite their small magnitude, to produce a bright signal away from the device curve. By applying a dephasing gradient in the slice direction, spins that are far away from each other are effectively nulled and only those that are close to each other and the device coil produce a bright signal.

In-plane rotation is then used to reduce data requirements. It is easy to see from Figures 2 and 3 that the more horizontal the projection image is the more efficiently the copies can be packed without overlap. This optimal in-plane rotation angle is found by searching over a uniformly distributed sparse set of rotation angles.

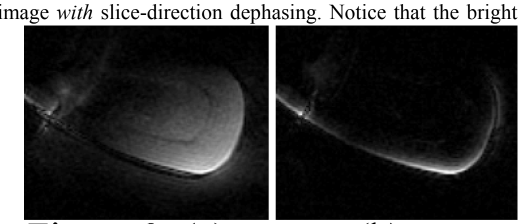
Figure 3: (a) (b)

The method was tested by inserting an active loopless guidewire into an aortic phantom (Shelly Medical Imaging Technologies, London, Canada). As online adaptive data gathering has not been implemented on the MR scanner, the adaptive data gathering was simulated from full 3D k-space data. The guidewire was positioned at twenty six adjacent positions in the phantom and at each position a full 3D k-space data set was collected. All projection data was collected by sampling on 2D-planes in 3D k-space. The slice-direction dephasing was achieved by offsetting the 2D-plane away from the origin of 3D k-space.

Results: The curve of the device was successfully computed in all the positions in the experiment. Figure 4 displays the results of one position. The estimated 3D curve of the device is re-projected and overlaid, in green, onto the two actual undersampled, slice-dephased, projection views used (in grayscale). Notice that estimated curve matches the projection image of the device.

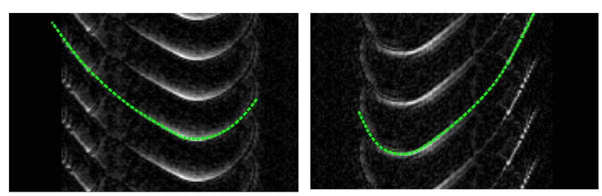
Figure 4: (a) (b)

Discussion: By adapting the orientation of projection views of an active device to the current estimate of the device trajectory and exploiting the sparsity and simplicity of these images, the amount of data necessary for the estimation of the trajectory of a moving active device is vastly reduced. This allows for the incorporation of the dynamic tracking of active devices into a real-time MRI visualization system for use in interventional procedures.

Compressed-sensing-based image-reconstruction methods are able to reduce the data required to reconstruct an (NxN) sparse image to O(K) where K is the number of non-zero pixels in the expected sparse image. In active-device projection imaging K~O(N) and therefore the data reduction is O(N). In our method we exploit the fact that the image is not merely sparse but also of reduced spatial extent; in particular the extent of the field of view in the phase-encoding direction is O(1). Consequently we are able to use traditional Fourier-domain undersampling (and vastly cheaper computation) to also achieve a data reduction of O(N).

References: 1.Guttman JMRI 26:1429-1435(2007) 2.Kocaturk JMRI 30:461-465 (2009) 3. Dumoulin MRM 63:1398-1403 (2010) 4. George MRM 63:1070-1079 (2010) 5. Schirra MRM 64:167-176 (2010) 6. George SCMR p.249 (2010) 7. Derbyshire JMRI 8:924-932 (1998)